EGYPTIAN JOURNAL OF BOTANY (EJBO)

Eco-sustainable synthesis, characterization, and biotechnological applications of zirconia nanoparticles and their nanocomposites: An overview

Medhat A. Abu-Tahon[1], Mohamed Ghareib[2], Manal M. Housseiny[2], Ismail M. Shahhat[1], Ahmad M. Abdel-Majeed[1], Yahia H. Ali[1], Intisar K. Saeed[1], Muaz M. Abdellatif[1]

[1]*Biological Science Department, Faculty of Science, Northern Border University, Arar, Saudi Arabia*

[2]*Biological and Geological Sciences Department, Faculty of Education, Ain Shams University, Roxy, Heliopolis, P.C.11757, Cairo, Egypt*

ARTICLE HISTORY

Submitted: February 24, 2025

Accepted: July 3, 2025

CORRESPONDANCE TO:

Medhat Ahmed Abu-Tahon

Department of Biological Sciences, College of Science, Northern Border University, Arar, Saudi Arabia

Email: medhatahon@gmail.com

DOI: 10.21608/ejbo.2025.360497.3196

EDITED BY: Neveen Mahmoud Khalil

REVIEW ARTICLE

Nanoscience and nanotechnology offer potential solutions to environmental pollution and climate change which are the major global challenges. Both chemical and physical approaches are employed for the creation of nanoparticles; however, biological approaches are favored for their eco-friendliness, cleanliness, safety, cost-efficiency, user-friendliness, and effectiveness in ensuring high productivity and purity. In this review, we explore the biosynthesis of ZrO_2NPs utilizing bacteria, fungi, and plants. Bioactive metabolites released by these organisms, such as polyphenols, fucoidans, flavonoids enzymes, reducing sugars, amino acids, and saponins play an important part in bioreduction, biocapping, and biostabilization processes. Various approaches are employed for the recognition and characterization of biosynthesized nanoparticles such as UV–vis spectroscopy, TEM, FT-IR, DLS, SEM, XRD, zeta potential assessment, etc. Green ZrO_2NPs have remarkable features, including a nanoscale size of 5-50nm and various morphologies e.g. nanospheres, nanochains, and nanorods, and broad bandgap energy of 3.7–5.5eV. Their great stability and biocompatibility make them useful for biological and environmental applications including pathogen and cancer deactivation, and pollution elimination. Green ZrO_2-based nanocomposites have emerged as promising materials for water treatment, anti-biofilms, nanoelectronic devices, and catalytic reduction. The final portion includes possible applications, a summary, and upcoming challenges.

Keywords: Biomedical applications, Characterization, Environmental remediation, Green synthesis, Zirconia nanoparticles

INTRODUCTION

Nanotechnology refers to the capability to monitor, quantify, modify, and synthesize materials at the atomic or molecular level, typically within the range of 1 to 100 nanometers. The distinct structural and chemical of metallic nanoparticles, tiny size, surface charge, surface chemistry, and high surface-to-volume ratio present a substantial prospect for extensive nanomaterial deployments in biotechnology, electronics, environmental remediation, optics, and medicine (Kumari et al., 2022). There are two primary methods for synthesizing nanoparticles, the top-down approach and the bottom-up approach. In the top-down approach, nanoparticles are created by minimizing the size of bulk materials through various methods. In contrast, the bottom-up approach involves assembling smaller building blocks into a larger structure (Saif et al., 2016).

There are various physical and chemical methods to produce zirconia nanoparticles (ZrO_2NPs). These methods include microwave plasma, laser ablation, hydrothermal techniques, thermal decomposition, and sol–gel methods (Chau et al., 2023). These methods are widely employed to produce metal and metal oxide nanoparticles. Nevertheless, this production necessitates the use of highly reactive and toxic reduced agents, such as sodium borohydride and hydrazine hydrate, which have harmful effects on the environment (Saif et al., 2016).

Scholars are now focused on biological pathways for economic and easy manufacturing of nanoparticles due to the distinct constraints of physical and chemical procedures. These include the biosynthesis of NPs at moderate pH, temperature, and pressure, which does not need toxic or hazardous compounds and avoids the inclusion of external reducing, capping, and stabilizers. Additionally, the green synthesis of nanoparticles is energy-efficient, cost-effective, and can be easily scaled up for Mass production (Usman et al., 2019).

Zirconium dioxide nanoparticles (ZrO_2NPs) have garnered significant research interest among transition metal oxide nanoparticles due to their distinctive catalytic, mechanical, sensing, biocompatible, optical, thermal, and electrical capabilities (Kirubakaran et al., 2025). Additionally, ZrO_2 can exist in different crystalline phases, monoclinic, tetragonal, and cubic determined by the synthesis methods used (Shinde et al., 2018).

Zirconium dioxide nanoparticles are typically synthesized using a variety of chemical and physical techniques, such as aqueous precipitation, the sol-gel process, microwave plasma, laser ablation, and hydrothermal methods (Majedi et al., 2016). These methods for synthesizing ZrO_2NPs involve the use of toxic chemicals, expensive equipment, and energy-intensive processes to achieve crystallinity (Majedi et al., 2016). Various reducing agents, including bacteria, fungi, and plants have been utilized in the green synthesis of ZrO_2NPs (Elsayed et al., 2022; Safaei et al., 2022; Weng et al., 2025). Antibiotic resistance is a major issue for Population health across the world. The overuse of antibiotics to treat the infection of bacteria in humans and aquatic animals has resulted in the spread of various antibiotic-resistant strains in the environment (Elshobary et al., 2025). Multidrug-resistant microorganisms present a significant global public health threat, as they are responsible for numerous potentially fatal infectious diseases caused by pathogenic bacteria (Selvam et al., 2023). Due to mutations, changing environmental conditions, and extensive drug usage, the number of multidrug-resistant bacterial strains is steadily increasing (Chelliah et al., 2023). To address antibiotic resistance, researchers are developing new medications to treat microbial infections. Biosynthesized ZrO_2NPs show promise as unique and potent agents against multidrug-resistant pathogens due to their non-toxic nature and strong antibacterial properties. Recent studies have demonstrated that biosynthesized ZrO_2NPs can effectively control a variety of pathogenic microorganisms (Elsayed et al., 2022; Chau et al., 2023).

This review highlights the simple and swift biological synthesis of ZrO_2NPs utilizing both microorganisms and plants, along with their characterization. It also explores their potential applications in antimicrobial activity, cytotoxicity, water purification, dental implants, and solar cells.

Biosynthesis of ZrO_2NPs

The green synthesis of nanoparticles neglects various harmful aspects by enabling their production under mild pressure, temperature, and pH conditions, all while being significantly more cost-effective (Ahmed et al., 2021a). Additionally, relative to chemically or physically produced nanoparticles, biosynthesized nanoparticles have much better antibacterial activity and are more biocompatible (Vennila et al., 2018). For these reasons, researchers are concentrating increasingly on employing various biological resources to synthesize ZrO_2NPs in a safe, efficient, and environmentally friendly manner (Elsayed et al., 2022; Chowdhury et al., 2023). Microbe-mediated nanoparticles have recently attracted considerable attention due to the widespread availability of microorganisms, their ease of reproduction, and their safe use in the biosynthesis process (Salem & Fouda, 2021). Microbial synthesis of nanoparticles involves the use of microorganisms, including bacteria and fungi, which can significantly contribute to the reduction and stabilization processes (Xie, 2025).

A variety of plant extracts are being used as eco-friendly stabilizing agents in the synthesis of ZrO_2NPs. The plant-mediated synthesis of metal oxide nanoparticles is gaining significant attention owing to their simplicity and quick production of nanoparticles with diverse morphologies, and the eradication of the need for specific maintenance of cell cultures (Gowri et al., 2015). For the biosynthesis of ZnO_2NPs, various parts of plants such as leaves, roots, fruits, and flowers can be utilized. Figure 1 shows the various steps of eco-friendly biosynthesis of ZrO_2NPs using microbial culture supernatant, microbial cell free filtrate, and plant extracts and their potential applications.

Fungi-mediated biosynthesis of ZrO_2NPs

The use of fungi to produce ZrO_2NPs presents several advantages. Firstly, they can withstand severe formation conditions, such as strong pressure in the flow and agitation in bioreactors, making them well-suited for the manufacture of ZrO_2NPs (Ghomi et al., 2019). Fungi exhibit rapid growth that can be controlled by adjusting their nutrient sources. As a result, they generally show greater resilience to genetic and ecological mutations, which enhances the cultivation approach (Gowri et al., 2014) These characteristics make fungi more suitable for the biosynthesis of ZrO_2 compared to other biological fabrication strategies, such as those involving bacteria and plants (Tran et al., 2022). Nanoparticles can be synthesized through both extracellular and intracellular pathways (Ghomi et al., 2019; Elsayed et al., 2022).

The culture supernatant of microorganisms is rich in various bioactive compounds, such as amino acids, proteins, enzymes, and other macromolecules. These compounds function as agents for reduction, capping, and stabilization throughout the synthesis process (Huq & Akter, 2021). The intracellular pathway involves transporting metal ions inside the cell through interactions with the negatively charged receptors on the cell wall, subsequently the reduction of these ions by the cellular enzymes. On the other hand, the extracellular production of nanoparticles is promoted by nitrate reductase, which helps in the reduction of zirconium ions (Figure 2). The creation of nanoparticles occurs through nucleation, aggregation, and subsequent growth (Ahmed et al., 2021a). The reduction of Zr4+ by biological means probably starts with the transfer of electrons from NADH through an NADH-dependent reductase, which acts as an electron shuttle. This enables Zr^{4+} to receive an electron, transforming it into Zr^{o}, and leading to the formation of ZrO_2NPs (Mohd Yusof et al., 2019). Numerous recent studies have concentrated on the cost-effective biosynthesis of ZrO_2NPs using different fungal species (Table 1). Elsayed et al. (2022) recorded the biosynthesis of zirconia nanoparticles by using the fungal biomass of *Fusarium oxysporum* to reduce potassium hexafluorozirconat (K_2ZrF_6) as a precursor.

A notable change in color from pink to purple served as an initial indicator of zirconia nanoparticle synthesis. Ghomi et al. (2019) reported the synthesis of zirconia nanoparticles by using zirconium tetrachloride ($ZrCl_4$) as a precursor and the culture supernatant of *Penicillium aculeatum* observing a color transition from pale yellow to deep yellow as a preliminary sign of nanoparticle formation. Ahmed et al. (2021a) demonstrated the synthesis of zirconia nanoparticles using *Enterobacter* sp. by using zirconium chloride octahydrate ($ZrOCl_2 \cdot 8H_2O$), where the formation of visible precipitated clusters indicated the onset of nanoparticle biosynthesis.

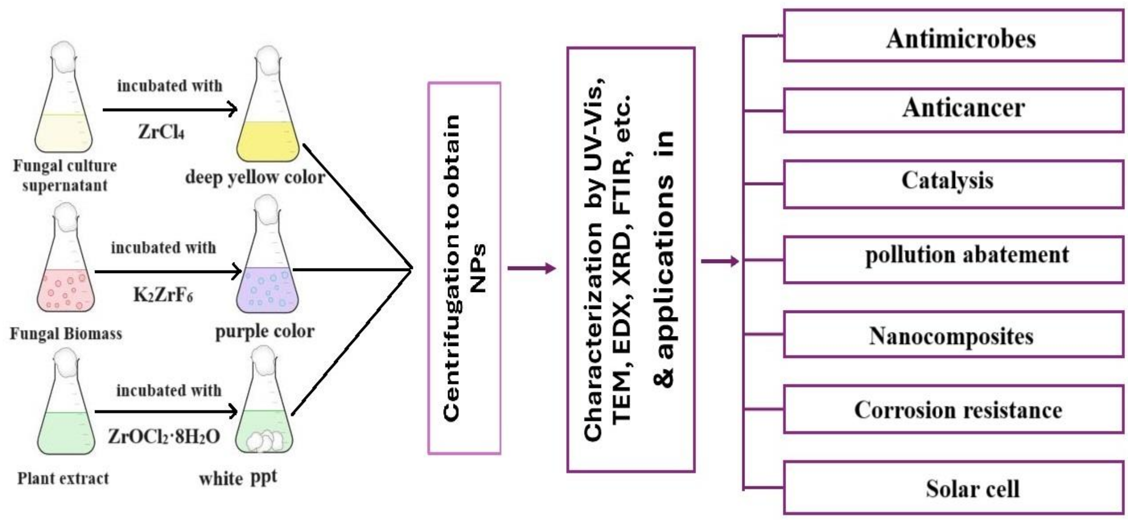

Figure 1. Schematic illustration of biosynthesis and prospective applications of zirconia nanoparticles

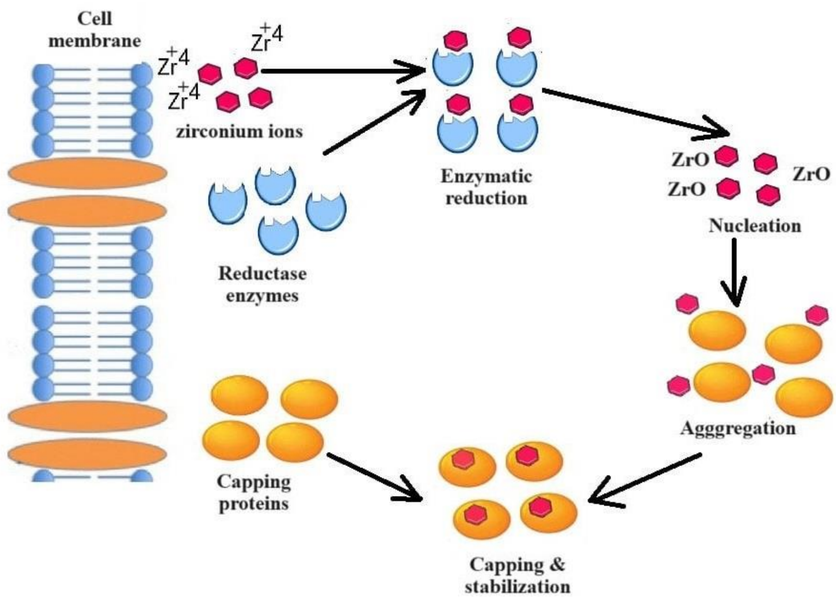

Figure 2. Schematic illustration of the mechanism of extracellular synthesis of zirconia nanoparticles by microbial cells

Table 1. Summary of the different microorganisms used in biosynthesis of zirconium nanoparticles

Microorganism	Zirconia source	Synthesis conditions (Salt con., temperature, incubation time, pH, agitation speed)	Size range, average size (nm)	Shape	Surface chemistry	Crystal phase	Reference
Fusarium oxysporum (biomass)	K_2ZrF_6	0.1mM, 25°C, 24h, pH 9, 180 rpm	5 - 15	Spherical	Hydroxyl, carbonyl, amine, alkene	Not recorded	Elsayed et al. (2022)
Fusarium solani (culture supernatant)	$Zr(NO_3)_4$	28 °C, 5 h, pH 6.8	30-40	Spherical	Hydroxyl, carbonyl	Tetragonal	Kavitha et al. (2020)
Penicillium spp. (culture supernatant)	$ZrCl_4$	0.5mM, 28°C, 7 days, pH 9, 120 rpm	< 100	Spherical	Hydroxyl, carbonyl, amine	Not recorded	Ghomi et al. (2019)
Humicola sp. (biomass)	K_2ZrF_6	0.1mM, 50°C, 96h, pH 9, 200 rpm	11	Quasi-spherical	Hydroxyl, carbonyl, amine	Not recorded	Uddin & Ahmad (2016)
Fusarium oxysporum (biomass)	K_2ZrF_6	0.1mM, 27°C, 4h, pH 3.6, 200 rpm	7.3	Spherical	Hydroxyl, amine	Monoclinic	Bansal et al. (2004)
Halomonas elongata (culture supernatant)	$ZrCl_4$	0.23mM, 32 °C, 72h, 120 rpm.	55-60	Spherical	Hydroxyl, carboxyl	Monoclinic	Safaei et al. (2022)
Enterobacter sp. (culture supernatant)	$ZrOCl_2 \cdot 8H_2O$	5mM, 30 °C, 24h, 150 rpm	30-75	Spherical	Hydroxyl, alkene	Not recorded	Ahmed et al. (2021a)
Pseudomonas aeruginosa (culture supernatant)	$ZrOCl_2 \cdot 8H_2O$	20mM, 37°C, 96 h, pH 7.4	15	Spherical	Hydroxyl, carboxyl	Monoclinic & tetragonal	Debnath et al. (2020)
Acinetobacter sp. (culture supernatant)	$ZrOCl_2 \cdot 8H_2O$	100mM,60 °C, 20 min, pH 2,150 rpm	44	Spherical	Hydroxyl, carbonyl	Monoclinic & tetragonal	Suriyaraj et al. (2019)

Bacteria-mediated biosynthesis of ZrO_2NPs

The proficiency of bacteria in nanoparticle biosynthesis stems from their ability to thrive and grow rapidly in challenging environments, leveraging their natural resistance mechanisms such as oxidation-reduction processes, intra/extracellular metal precipitations, pH balancing, and enzymatic volatilization of metals (Ahmed et al., 2021b). During metabolic processes, bacteria release enzymes and proteins both intracellularly and extracellularly, which may facilitate the biological reduction and biochemical stabilization of zirconium ions (Debnath et al., 2020). The release of macromolecules, such as proteins rich in negative charge-bearing groups, enhances the chemical characteristics of the bacterial cell surface (Suriyaraj et al., 2019).

The process of forming ZrO_2 nanoparticles through bacterial cells involves several intricate steps, including (i) the biosorption of zirconium ions onto the cell surface, which occurs via various physical and chemical interactions such as hydrogen linkage electrostatic forces, ionic exchange, and chelation, and (ii) the bioreduction and biostabilization facilitated by secondary metabolites produced during the lag phase of bacterial growth in culture media (Safaei et al., 2022). Numerous studies have shown the cost-effective biosynthesis of ZrO_2NPs using various bacterial strains (Table 1). Safaei et al. (2022) recorded extracellular biosynthesis of zirconia nanoparticles by using the culture supernatant of *Halomonas elongata* bacterium to reduce zirconium chloride as a precursor. Zirconium nanoparticles showed a peak absorbance at 275 nm in UV-vis spectroscopy. Ahmed et al. (2021a) successfully synthesized zirconia nanoparticles extracellularly by reduction of $ZrOCl_2 \cdot 8H_2O$ using *Enterobacter* sp. zirconia nanoparticles exhibited peak absorbance at 256nm in UV-vis spectroscopy. Debnath et al. (2020) recorded the biosynthesis of zirconia nanoparticles by using the culture supernatant of *Pseudomonas aeruginosa* to reduce $ZrOCl_2 \cdot 8H_2O$ as a precursor. The change of color from colorless to white was a preliminary sign of zirconia nanoparticle biosynthesis. Zirconia nanoparticles exhibited peak absorbance at 256nm in UV-vis spectroscopy.

Plants-mediated biosynthesis of ZrO_2NPs

The green biosynthesis of zirconia nanoparticles through biomolecules derived from plant extracts can take place in a limited time, whereas microbial processes typically extend over numerous days at ambient conditions (Selvam et al., 2023). Plant extracts contain various metabolites and phytochemicals that enhance the kinetics of the ZrO_2 production process and boost their biological activities (Chelliah et al., 2023). Currently, extracts from different plant parts such as roots, leaves, flowers, and fruits are employed in the biosynthesis of ZrO_2NPs. Several phytochemicals, including flavones, amides, aldehydes, ketones, terpenoids, sugars, and carboxylic acids play a crucial role in the reduction of metal precursors (Kumari et al., 2022). Figure 3 shows a diagrammatic demonstration of the method by which these bioreductant molecules reduce the metal precursor to synthesize zirconia nanoparticles. Phytochemicals function as bioreductants, reducing Zr^{4+} to form the octahedral complex $[Zr(H_2O)_6]^2$. This improves stability and prevents zirconium complexation from clustering when chelating with Zr^{2+}–phytochemicals. The calcination of Zr^{2+}–phytochemicals complex yields ZrO_2NPs with the release of N_2, CO_2, H_2O, and many degradation products (da Silva et al., 2019).

The initial stage in the extraction process for the biosynthesis of zirconia nanoparticles involves gathering the appropriate plant part (such as leaves, roots, flowers, or seeds) and rinsing it with distilled water. The second stage in the biosynthesis process involves the reduction of zirconia precursors by the phytochemicals in the plant extract. The extraction process was conducted using both dried plant material (da Silva et al., 2019; Chau et al., 2023; Muthulakshmi et al., 2023b) and fresh plant materials (Al-Zaqri et al., 2021; Chowdhury et al., 2023). Phytochemical extraction is typically carried out with various solvents, including water, ethanol, and hexane. (Alagarsamy et al., 2022).

Water was the most used solvent for extracting botanical parts during the biosynthesis of zirconia nanoparticles (Shinde et al., 2018; da Silva et al., 2019; Al-Zaqri et al., 2021; Chowdhury et al., 2023; Muthulakshmi et al., 2023b). Additionally, ethanol was sometimes employed for extraction in the biosynthesis of zirconia nanoparticles from certain plant parts (Davar et al., 2018). Various plant parts have been utilized in the biosynthesis of ZrO_2NPs (Table 2). The most prevalent zirconia precursor was $ZrOCl_2 \cdot 8H_2O$ which is reduced into the complex of Zr^{+2} -phytochemicals complex (Muthulakshmi et al., 2023b). The final step in the biosynthesis of zirconium nanoparticles involves thermal calcination at a high temperature range of 500–800°C for 2–4h, converting the complex into ZrO_2NPs (Chau et al., 2023).

Table 2 Summary of the different plants used in biosynthesis of zirconia nanoparticles

Plant	Zirconia source	Synthesis conditions (salt con., temperature, incubation time, pH, agitation speed	Size range, average size (nm)	Shape	Surface chemistry	Crystal phase	Reference
Azadirachita indica (leaf extract)	$Zr(NO_{3)}$**4**	0.5M, 80°C, 3-4h, 200 rpm	16	Spherical	Hydroxyl, alkene, & amide	Tetragonal	Singh et al. (2025)
Sonchus asper (leaf extract)	$ZrOCl_2{\cdot}8H_2O$	0.1M, 70–80°C, 3-4h	5.9–7.8	Spherical	Hydroxyl, alkene	Not reported	Al-nayili & Idan (2023)
Thymus vulgaris (extract)	$Zr(SO_4)2$	100ml of, $Zr(SO_4)_2$ and 100ml of extract pH (10–12)	45.1	Spherical	Hydroxyl, alkene, & carbonyl	Not reported	Tharp & Karem (2024)
Laurus nobilis (Leaf extract)	$ZrOCl_2{\cdot}8H_2O$	0.1M, magnetic stirrer	20-100	Spherical	Hydroxyl, carboxylic acids, & alkane	Monoclinic tetragonal	Chau et al. (2023)
Murraya koenigii (leaf extract)	$Zr(NO_3)4$	0.1M $Zr(NO_3)_4$, 60min	27	Spherical	Hydroxyl, alkene, amide & carboxylic acid	Monoclinic	Chelliah et al. (2023)
Garlic (Bulb) &Ginger (rhizome)	$ZrO(NO_{3)}$**2**	10mM, 80°C, magnetic stirrer	4883 (garlic) 554 (ginger)	Spherical, triangular,irregular	carboxylic acid, amine, & alkene	Not reported	Chowdhury et al. (2023)
Parkia biglandulosa (leaf extract)	$ZrOCl_2{\cdot}8H_2O$	0.05M, 85°C, 10min, magnetic stirrer	5-13	Spherical	Hydroxyl, carbonyl, & alkyl	Not reported	Muthulakshmi et al. (2023a)
Guettarda speciosa (leaf extract)	$ZrO(NO_3)_2$	0.08M, 85°C, magnetic stirrer	6-9	Quasi-spherical Irregular	Hydroxyl, carbonyl, & alkyl	Monoclinic & tetragonal	Muthulakshmi et al. (2023b)
Annona reticulata (leaf extract)	$ZrOCl_2{\cdot}8H_2O$	10 mM, 30°C, 48h, 200 rpm	13-20	Spherical	Hydroxyl, carbonyl, & amine	Not reported	Selvam et al. (2023)
Sapindus mukorossi (pericarp extract)	$ZrOCl_2{\cdot}8H_2O$	0.1M ,60°C, 3-4h, magnetic stirrer	5	Spherical	Hydroxyl, alkyl, & amide	Not reported	Alagarsamy et al. (2022)
Phyllanthus niruri (leaf extract)	$ZrOCl_2{\cdot}8H_2O$	0.02M, 80°C, 3-4h	125.4	Spherical	Hydroxyl, alkane, & alkene	Monoclinic	Yuan et al. (2022)

Table 2. Cont.

Plant	Zirconia source	Synthesis conditions (salt con., temperature, incubation time, pH, agitation speed	Size range, average size (nm)	Shape	Surface chemistry	Crystal phase	Reference
Wrightia tinctoria (leaf extract)	$ZrOCl_2·8H_2O$	0.1M, 75 °C, 3-4h, magnetic stirrer	17	Spherical	Hydroxyl, alkyl, & carboxylic acid	Monoclinic & tetragonal	Al-Zaqri et al. (2021)
Helianthus Annuus (seed extract)	$ZrOCl_2·8H_2O$	0.05M, 23h, magnetic stirrer	35.4	Spherical	Carboxyl, alkyl, alkene, & amide	Monoclinic	Goyal et al. (2021)
Euclea natalensis (root extract)	$ZrOCl_2·8H_2O$	0.03M, 3h	5.9–8.5	Spherical	Hydroxyl, alkene, & carboxyl	Monoclinic& tetragonal	da Silva et al. (2019)
Salvia Rosmarinus (leaf extract)	$ZrOCl_2·8H_2O$	0.03M, 70°C, 1h, magnetic stirrer	12–17	Semi-spherical	Hydroxyl, carboxyl, & alkyl	Cubic	Davar et al. (2018)
Ficus benghalensis (leaf extract)	$ZrOCl_2·8H_2O$	0.1M, microwave 15min, magnetic stirrer	14.7	Spherical	Hydroxyl, alkyl, & carbonyl	Monoclinic, tetragonal	Shinde et al. (2018)
Lagerstroemia speciosa (leaf extract)	$Zr(NO_3)_4$	0.2M, 90°C, 3h, magnetic stirrer	56.8	Oval	Hydroxyl, carbonyl, & amine	Tetragonal	Saraswathi & Santhakumar (2017)
Acalypha Indica (leaf extract)	$ZrOCl_2·8H_2O$	0.1M, 80°C, 2h	20-100	cubic	Hydroxyl, alkyl, & amide	Monoclinic	Tharani (2016)
Citrus aurantifolia (fruit extract)	$Zr(CH_3COO)_4$	0.04M, 3h, pH 4, magnetic stirrer	21	Not reported	Hydroxyl, carboxylic, & ester	Not reported	Majedi et al. (2016)
Nyctanthes arbor-tristis (flower extract)	$ZrOCl_2·8H_2O$	0.4M, 2h	<150	Nanoflake	Not reported	Tetragonal	Gowri et al. (2015)
Aloe vera (leaf extract)	$ZrOCl_2·8H_2O$	0.4M, 4h	<50	spherical	Hydroxyl, carbonyl, & hydroxyl	Tetragonal	Gowri et al. (2014)
Aloe vera (leaf extract)	$ZrOCl_2·8H_2O$	10mM, 30°C, 48h	18-42	Not reported	Hydroxyl, carbonyl amide, & alkane,	Face centered cubic	Prasad et al. (2014)

The production of zirconia nanoparticles through the reduction of $Zr(NO_3)_4$ using *Azadirachita indica* leaf extract was reported by Singh et al. (2025). The initial white metal salt solution gradually turned light yellow, indicating the formation of ZrO_2NPs. Moreover, the extract of *Sonchus asper* leaves was utilized to reduce $ZrOCl_2 \cdot 8H_2O$, leading to the formation of ZrO_2NPs. The color change from brown to white served as an indication of the successful biosynthesis of zirconia nanoparticles (Al-nayili & Idan, 2023). Chowdhury et al. (2023) reported the biosynthesis of zirconia nanoparticles through the reductive action of ginger and garlic extracts, using $ZrO(NO_3)_2$ as a precursor. The initial change from light blue to white served as a preliminary indication of zirconia nanoparticle formation. In addition, the biosynthesis of zirconia nanoparticles was performed by the reductive effect of *Aloe vera* gel extract to $ZrOCl_2 \cdot 8H_2O$, and the preliminary sign of zirconia nanoparticles biosynthesis was the formation of turbid white colloidal particles (Gowri et al., 2014).

Culture and reaction conditions affecting zirconia nanoparticles biosynthesis

Several key parameters have been reported to influence the yield, production rate, morphology, and stability of biosynthesized zirconia nanoparticles, including: the type of culture media for microbes or plants mediated biosynthesis process, metal salt precursor (type & concentration), pH, incubation time, temperature, and stirring or shaking speed (Khandel & Shahi, 2018).

Maltose glucose yeast peptone medium (MGYP) was recorded as the optimal medium for biosynthesis of zirconia nanoparticles synthesized by *Fusarium oxysporum* (Elsayed et al., 2022) and *Humicola* sp. (Uddin & Ahmad, 2016). Moreover, Czapek's-dox medium was chosen for the biosynthesis of zirconia nanoparticles by *Fusarium solani* (Kavitha et al., 2020) and *Penicillium* spp. (Ghomi et al., 2019). While nutrient broth media was recorded for production of zirconia nanoparticles by *Enterobacter* sp. Ahmed et al. (2021a) and tryptone soya broth was recorded for *Pseudomonas aeruginosa* (Debnath et al., 2020).

Higher concentrations of botanical extracts and metal salts typically result in greater nanoparticle yields, though there may be a point at which further increases in concentration have minimal impact (Huq et al., 2023). May studies demonstrated the impact of different concentrations of metal salt precursor on the productivity of zirconia nanoparticles (Tables 1, 2). Ahmed et al. (2021a) reported that a concentration of 5 mM of $ZrOCl_2 \cdot 8H_2O$ caused a high yield in zirconia nanoparticles biosynthesis by *Enterobacter* sp. compared to other tested concentrations (0.5, 1.0, 3, and 10mM). A 1.5mM concentration of $ZrCl_4$ resulted in greater zirconia nanoparticle production by *Penicillium* spp. compared to a 0.5mM concentration of same salt (Ghomi et al., 2019). Moreover, a concentration of 0.05M of $ZrOCl_2 \cdot 8H_2O$ showed a higher yield in zirconia nanoparticles formation by *Parkia biglandulosa* leaf extract compared to other concentrations (0.01 & 0.03M) (Muthulakshmi et al., 2023a).

Time to reaction may be utilized to manipulate the size and form of green NPs. It has been documented in the literature that the reaction time required for plant-mediated synthesis of zirconia nanoparticles is shorter than that for fungi-mediated synthesis (Tables 1, 2). The time needed to biosynthesis of zirconia nanoparticles from *Parkia biglandulosa leaf* extract was about 10min (Chowdhury et al., 2023).While, the biosynthesized zirconia nanoparticles by *Penicillium* spp. culture supernatant needed about 7 days (Ghomi et al., 2019). Moreover, the reaction time reached about 4 and 3 days for the biosynthesized zirconium nanoparticles from *Humicola* sp. biomass and *Halomonas elongata* culture supernatant, respectively (Uddin & Ahmad, 2016) and (Safaei et al., 2022), respectively. Additionally, the recorded reaction times for the biosynthesis of zirconium nanoparticles using *Ficus benghalensis* leaf extract and *Acinetobacter* sp. culture supernatant were approximately 15min and 20min, respectively (Shinde et al., 2018) and (Suriyaraj et al., 2019), respectively. The reaction time required for plant-mediated synthesis of zirconia nanoparticles generally ranges from 2 to 4h (Gowri et al., 2014; Prasad et al., 2014; Gowri et al., 2015; Saraswathi & Santhakumar, 2017; da Silva et al., 2019; Al-Zaqri et al., 2021; Alagarsamy et al., 2022; Chowdhury et al., 2023).

The pH value can influence the velocity of particle formation, with more basic or acidic conditions typically resulting in higher reaction speeds (Yazdanian et al., 2022). Alkaline conditions promote the proton dissociation and stimulation of phytochemicals in plants, whereas lower pH levels keep them predominantly protonated. This results in reduced reducing or capping activity during nanoparticle synthesis (Din et al., 2018).

Different pH values were recorded for zirconia nanoparticles biosynthesis by different resources (Tables 1, 2). The yield of biosynthesized zirconia nanoparticles by *Penicillium* spp. culture supernatant is significantly influenced by the pH values of the culture conditions. The highest yield was observed at pH 9, compared to yields at pH 6, 7, and 8 (Ghomi et al., 2019). Alkaline pH values were recorded for zirconia nanoparticles biosynthesis by different resources (Uddin & Ahmad, 2016; Elsayed et al., 2022). Studies indicate that the suppression of plant phytochemicals in acidic environments is evidenced by the absence of nanoparticle (NP) formation at very low pH levels. On the contrary, Bansal et al. (2004) reported that the ability of *Fusarium oxysporum* to reduce K_2ZrF_6 to form zirconia nanoparticles at pH 3.6. Also, plant extract of *Citrus aurantifolia* can reduce $Zr(CH_3COO)_4$ to form zirconia nanoparticles at pH 4 (Majedi et al., 2016). While weakly acidic pH value was also reported for zirconia nanoparticles biosynthesis by *Fusarium solani* at pH 6.8 (Kavitha et al., 2020). In general, nanoparticles (NPs) formed in an alkaline reaction medium tend to be smaller and exhibit greater stability. This may be attributed to a more efficient capping process that occurs earlier at alkaline pH values, facilitated by a higher concentration of activated phytochemicals (Miu & Dinischiotu, 2022).

An increase in reaction temperature results in greater kinetic energy for the biomolecules involved in the reduction process, leading to a more rapid consumption of metallic ions and, consequently, a larger yield of nanoparticles (Miu & Dinischiotu, 2022). Additionally, it has been established that higher temperatures tend to produce smaller particles, as observed in certain fungi and most plant extracts used in the biosynthesis of zirconia nanoparticles. *Humicola* sp. biomass which mediated synthesis of zirconia nanoparticles, recorded a particle size of 11nm at 50^{o}C (Uddin & Ahmad, 2016). Moreover, this fact was confirmed experimentally by a series of studies in plant extracts- mediated synthesis of zirconia nanoparticles (Tharani, 2016; Davar et al., 2018; Al-Zaqri et al., 2021; Alagarsamy et al., 2022). On the contrary, small sized zirconia nanoparticles (5-15nm) were synthesized at low temperature 25^{o}C by *Fusarium oxysporum* (Elsayed et al., 2022) and a particle size of 7.3nm was recorded at 27^{o}C by another isolate of *Fusarium oxysporum* (Bansal et al., 2004).

The shaking speed is crucial for maintaining the motion of reactants and enhancing the likelihood of metal ions colliding with biomolecules in a constantly agitated mixture. Thus, the rate of the green synthesis reaction should be directly proportional to the agitation speed (Miu & Dinischiotu, 2022). Most previous reports on biosynthesized zirconia nanoparticles using microbial biomass or culture supernatant highlight the significance of shaking velocity as a crucial reaction condition during the nanoparticle synthesis process (Ghomi et al., 2019; Suriyaraj et al., 2019; Ahmed et al., 2021b; Elsayed et al., 2022; Safaei et al., 2022). Additionally, a considerable amount of prior research on the biosynthesis of zirconia nanoparticles using plant extracts has confirmed that the use of a magnetic stirrer is one of the key reaction conditions in the biosynthesis process (Davar et al., 2018; Al-Zaqri et al., 2021; Chau et al., 2023; Muthulakshmi et al., 2023a, b).

Characterization of biosynthesized ZrO_2NPs

Numerous studies in literature have extensively documented the characterization of biosynthesized zirconia nanoparticles using a variety of analytical techniques, including UV-visible spectrophotometry, scanning electron microscopy (SEM), X-ray diffraction (XRD), transmission electron microscopy (TEM), Fourier-transform infrared spectroscopy (FTIR), dynamic light scattering (DLS), and zeta potential analysis. These techniques offer essential insights into the physical and chemical characteristics of nanoparticles, such as their size, shape, surface functional groups, crystallinity and surface charge.

UV-visible spectrophotometry is frequently employed to analyze the optical properties of ZrO_2NPs, including their absorption spectra and bandgap energy. In ZrO_2, as with any other semiconductor, the excitation energy corresponds to the energy required to transfer an electron from the valence band to the conduction band. This transition is detected spectrophotometrically as an absorption peak . The energy value of this peak is known as bandgap value. The slight variation in the absorption peak for biosynthesized zirconia nanoparticles is attributed to the different intermediate electronic levels created by impurities or lattice defects (Abdo et al., 2021). The most frequently recorded absorption peak was at 275nm (Shinde et al., 2018; Goyal et al., 2021; Alagarsamy et al., 2022; Elsayed et al., 2022; Safaei et al., 2022). A further absorption peak was reported at

213nm (Gowri et al., 2014; Majedi et al., 2016). Moreover, zirconia nanoparticles biosynthesized by *Guettarda speciosa* leaf extract showed a absorption beak at 226nm (Muthulakshmi et al., 2023b) and that biosynthesized by *Nyctanthes arbor-tristis* flower extract showed a absorption beak at 234nm (Gowri et al., 2015). Additional absorption peaks were recorded in the range of 256-263nm (Ahmed et al., 2021a; Muthulakshmi et al., 2023a). Moreover, higher absorption peaks were also recorded in the range of 300-374nm (Saraswathi & Santhakumar, 2017; Al-Zaqri et al., 2021; Chau et al., 2023). The highest absorption beak was recorded for zirconia nanoparticles biosynthesized by *Aloe vera* gel extract at a wavelength of 420nm (Prasad et al., 2014). Bandgap energy of the biosynthesized zirconia nanoparticles exhibited values ranging from 3.70-3.78eV, where the ZrO_2NPs biosynthesized by *Helianthus annuus and Wrightia tinctoria* recorded 3.70 and 3.78eV, respectively (Goyal et al., 2021) and (Al-Zaqri et al., 2021), respectively. The recorded bandgap energies for zirconia nanoparticles biosynthesized from various biological sources are as follows: *Ficus benghalensis* (4.9eV) (Shinde et al., 2018), *Parkia biglandulosa* (4.95eV) (Muthulakshmi et al., 2023a), *Nyctanthes arbor-tristis* (5.31eV) (Gowri et al., 2015), *Aloe vera* (5.4eV) (Gowri et al., 2014), *Guettarda speciosa* (5.49eV) (Muthulakshmi et al., 2023b), *Sapindus mukorossi* (5.53eV, (Alagarsamy et al., 2022), and *Citrus aurantifolia* (5.82eV) (Majedi et al., 2016).

The average particle size of ZrO_2NPs can be determined using various techniques, including XRD and TEM. The particle size of ZrO_2NPs varies from 5 to less than 150nm, with the majority of biosynthesized ZrO_2NPs falling within the 5 to 45nm range, as illustrated in Tables 1, 2. The smallest particle size (5nm) was recorded to the biosynthesized ZrO_2NPs by *Fusarium oxysporum* biomass (Elsayed et al., 2022), *Sapindus mukorossi* pericarp extract (Alagarsamy et al., 2022) and *Parkia biglandulosa* leaf extract (Muthulakshmi et al., 2023a). On the contrary, the biggest biosynthesized zirconium nanoparticles (4883nm) were synthesized by garlic bulb extract (Chowdhury et al., 2023). Small-sized ZrO_2NPs provide numerous biomedical advantages by enhancing their ability to penetrate cell walls, resulting in improved antibacterial, antifungal, and anticancer properties (Muthulakshmi et al., 2023a). In the nanoscale the particle size is inversely related to aggregation tendency.

The morphology of ZrO_2 nanocrystals produced via biological synthesis can be investigated using scanning or transmission electron microscopy analysis. For the biosynthesized ZrO_2NPs, a variety of diverse morphologies, including nanospheres, nanorods, nanoflakes nano-sized ovals and nanocubes were described (Tables 1, 2). Variation in reaction times can influence the size and shape of green-synthesized nanoparticles. As reaction time increases, both the particle size and the number of generated nuclei grow proportionally, however, if the reaction exceeds the optimal reduction time, the nanoparticles may begin to aggregate, leading to the formation of larger size (Yazdanian et al., 2022). The morphology of ZrO_2NPs is highly influenced by synthesis conditions, especially the ratio of the zirconium source to the green extract (Tran et al., 2022). The vast majority form of the microbial-mediated synthesis zirconia nanoparticles was the spherical (Bansal et al., 2004; Ghomi et al., 2019; Suriyaraj et al., 2019; Debnath et al., 2020; Kavitha et al., 2020; Elsayed et al., 2022; Safaei et al., 2022; Al-nayili & Idan, 2023; Tharp & Karem, 2024; Singh et al., 2025). While, in addition to their spherical morphologies, the ZrO_2NPs produced via plant extracts displayed a slight degree of shape variability. For example, oval-shaped biosynthesized zirconia nanoparticles obtained by *Lagerstroemia speciosa* leaf extract (Saraswathi & Santhakumar, 2017), cubic-shaped biosynthesized ZrO_2NPs using *Acalypha Indica* leaf extract (Tharani, 2016), and Nanoflake shaped nanoparticles obtained by *Nyctanthes arbor-tristis* flower extract (Gowri et al., 2015).

There are three typical crystalline phases for bulk ZrO_2NPs: monoclinic, tetragonal, and cubic (Tables 1, 2). The X-ray diffraction (XRD) analysis of green-synthesized ZrO_2 nanoparticles (ZrO_2 NPs) confirms their crystallinity and phase composition. The diffraction peaks, observed at $2\theta = 27.55–75.19°$, indicate that the synthesized ZrO_2 NPs exist in both monoclinic and tetragonal phases, with the (101) plane exhibiting high-intensity crystal formation (Muthulakshmi et al., 2023b). A monoclinic phase was recorded to ZrO_2NPs biosynthesized by *Halomonas elongata* culture supernatant which verified by the following planes −111, 111, 120, 022, and 131(Safaei et al., 2022). Additionally, monoclinic phase of ZrO_2NPs was biosynthesized by *Helianthus annuus* seed extract (Goyal et al., 2021) and *Acalypha Indica* leaf extract (Tharani, 2016). While a cubic phase was also recorded to biosynthesized ZrO_2NPs by *Salvia Rosmarinus* leaf extract with the following planes 111, 200, 220, 222, 311, and 400 (Davar et al., 2018). Tetragonal phase is one of the most prevalent single-crystal phases of biosynthesized ZrO_2NPs (Gowri et al., 2014, 2015; Muthulakshmi et al., 2023b; Saraswathi & Santhakumar, 2017). The most prevalent multiphase crystallinity of ZrO_2NPs is the two phases (monoclinic and tetragonal) which were reported to many biological producers (Shinde et al., 2018; da Silva et al., 2019; Suriyaraj et al., 2019; Debnath et al., 2020; Al-Zaqri et al., 2021; Chau et al., 2023).

FTIR can be used to characterize the surface chemistry of nanoparticles by identifying the organic functional groups present on their surface (Gowri et al., 2014). Different functional groups such as carbonyl, amine, carboxyl, and alkyl were recorded on the surface of ZrO_2NPs (Tables 1, 2). Antimicrobial properties of zirconia nanoparticles (ZrO_2NPs) can be enhanced by modifying or altering their surfaces through functionalization. Secondary products on a nanoparticle's surface may function as capping and stabilizing agents (Ghareib et al., 2019b; Abu-Tahon et al., 2020). Biomolecules that function as capping agents are significant because they stay connected to the exterior of particles, giving them durability over time. Moreover, the recorded absorption bands at 3416-3132, 2323, 1621, 1402, 1047, 961, 827, 649, and 465cm^{-1} indicate the presence of significant functional groups. Specifically, the broad band observed between 3416-3132cm^{-1} corresponds to moisture content during sample preparation (Gayathri & Balan, 2021), while the absorption band within 649-465cm^{-1} is characteristic of Zr–O–Zr vibrations. Additionally, peaks in the 1402-827cm^{-1} region confirm the presence of a Zr–O bond, supporting the tetragonal form of ZrO_2 NPs (Imanova et al., 2021). Furthermore, the peak at 1644cm^{-1} denotes O-H stretching and bending vibrations of absorbed water (Gayathri & Balan, 2021), whereas the peak at 1560cm^{-1} corresponds to adsorbed moisture (Singh & Nakate, 2014). Likewise, the band at 1456cm^{-1} represents hydrated molecules in the hydroxyl group (Zinatloo-Ajabshir & Salavati-Niasari, 2016), and the peak at 600cm^{-1} is attributed to Zr–O vibrations (Zinatloo-Ajabshir & Salavati-Niasari, 2016).

The zeta potential, determined by the surface charge, is essential for nanoparticle stability and plays a significant role in the primary adsorption of nanoparticles onto cell membranes (Hunter, 2013). Consequently, both the zeta potential and particle size play a role in determining the toxicity of nanoparticles (Hunter, 2013). Typically, suspensions of nanoparticles (NPs) with a zeta potential value below -25mV or above +25mV are stable because the strong electrostatic repulsion between highly charged surfaces prevents aggregation (Mourdikoudis et al., 2018). 36.5mV is the positive zeta potential value reported for the biosynthesized zirconium by *Acinetobacter* sp. (Suriyaraj et al., 2019) and *Enterobacter* sp. (Ahmed et al., 2021a). Moreover, different negative zeta potential values were recorded for the different biosynthesized zirconium, -32.8mV (Chau et al., 2023), -21.17mV (Al-Zaqri et al., 2021), -9.32mV (Goyal et al., 2021), -2.2, -3.87, and -1.72mV were recorded for the biosynthesized zirconium by different *Penicillium* spp. (Ghomi et al., 2019). The negative charge causes repulsion among the nanoparticles, which helps maintain their stability and prevents aggregation (Ghareib et al., 2019a; Abu-Tahon et al., 2024).

Biomedical applications of biosynthesized ZrO_2NPs

The biocompatibility and potential biomedical applications of zirconia nanostructures have been extensively studied. Research has shown that ZrO_2 nanostructures possess low cytotoxicity, rendering them appropriate for biomedical applications (Muthulakshmi et al., 2023b). Numerous studies have examined the potential toxicity of ZrO_2 nanostructures.

Antibacterial activity of biosynthesized ZrO_2NPs

Gram-positive bacteria have a thick peptidoglycan layer in their cell wall, whereas Gram-negative bacteria have a thin peptidoglycan layer (Yuan et al., 2022). Metallic nanoparticles tend to exhibit higher antibacterial effect towards Gram-negative bacteria in contrast to Gram-positive bacteria (Roy et al., 2019). The cause of this efficiency may be attributed to the presence of negative lipopolysaccharides (LPS), which facilitate adhesion to the cell wall of Gram-negative bacteria (Goyal et al., 2021). Due to electrostatic interactions, nanoscale size, large surface area, and excellent bioactivity, green ZrO_2NPs can easily penetrate cell membranes, disrupt key metabolic pathways, and finally cause the bacterial cells to become inactive (Al-Zaqri et al., 2021). Interestingly, nanoparticles interact with the plasma membrane lipid bilayer, resulting in membrane instability and loss of selective permeability, which allows some enzymes, proteins, ions, and nucleic acids to leak out of the cell (Roy et al., 2019). Once nanoparticles penetrate the bacterial cell, they interact with DNA, transforming it to a condensed form, thereby impairing its ability to replicate (Saraswathi & Santhakumar, 2017; Chelliah et al., 2023). Furthermore, nanoparticles can disrupt bacterial membranes through reactive oxygen species (ROS), particularly hydroxyl radicals (OH) which induces Phospholipid free radical damage and ultimately cause cell death (Chau et al., 2023).

Numerous publications have highlighted the impressive antibacterial properties of green ZrO_2NPs, demonstrating their effectiveness against both Gram-negative and Gram-positive bacteria (Table 3). For example, antibacterial activity of the biosynthesized ZrO_2NPs by *Azadirachita indica* leaf extract against *Escherichia coli* (Singh et al., 2025). Using the agar diffusion method, a zone of inhibition approximately 18 mm was observed. This inhibition is likely due to the deformation of the cell membranes and walls of *E. coli* caused by ROS generated by zirconium nanoparticles. Muthulakshmi et al. (2023b) investigated the antibacterial efficacy of the biosynthesized ZrO_2NPs from *Parkia biglandulosa* leaf extract against *Staphylococcus albus*, *Lactobacillus acidophilus*, and *Streptococcus mutans*. The zone of inhibition against *Lactobacillus acidophilus* was 28mm, against *Streptomyces albus* was 26mm and against *S. mutans* was 32 mm, all at a ZrO_2NPs concentration of 75 µg/ml. The study assumed that ROS generated by ZrO_2NPs inhibit bacterial cell growth via disrupting cell membranes, which increases barrier permeability, consequently, zirconia NPs can capture inside each cell.

Antifungal activity of biosynthesized ZrO_2NPs

The primary mechanism by which fungal cell division is disrupted may involve the production of ROS and free radicals by nanoparticles (Akintelu & Folorunso, 2020). Additionally, ergosterol in the fungal cell membrane can be harmed by NPs, which causes cell death (Allaker et al., 2012). The following are some possible pathways for metal nanoparticles' antimicrobial action: first, disruption of the cell wall and membrane; second, intracellular microbial component damage following cell wall rupture; and finally, the activation of oxidative damage (Salem & Fouda, 2021). ZrO_2NPs can alter the structural integrity of fungal cells by modifying physicochemical conditions, causing leaking of internal contents (Reddy et al., 2015). The resulting fungal death could be due to the inactivation of cellular enzymes and DNA, potentially through interactions with electron-donating groups like thiols, hydroxyls carbohydrates, indoles, amides, etc. (Dehghani & Haghighi, 2017) Many publications have reported the antifungal activity of biosynthesized ZrO_2 nanoparticles against fungal cells (Table 3).

The antifungal activity of the biosynthesized ZrO_2NPs from *Enterobacter* sp. culture supernatant against bayberry fungal pathogen *Pezicula versicolor* was reported (Ahmed et al., 2021a). Using the agar diffusion method, an antifungal inhibition zone of 25.18mm was observed at a 20µg/ml of ZrO_2NPs. Microscopy imaging techniques also revealed significant deconstruction of *P. versicolor* fungal cells, evidenced by exterior leakage of DNA and proteins. Additionally, numerous studies have reported both antibacterial and antifungal activities of green ZrO_2NPs from different microbes (Table 3). For example, Yuan et al. (2022) reported that biosynthesized ZrO_2NPs from *Phyllanthus niruri* leaf extract displayed valuable antibacterial activity against *B. subtilius, S. aureusm, K. pneumoniae* and *E. coli* in dose dependent style (50–200µg/ml) as shown in Table 3.

Anticancer activity of biosynthesized ZrO_2NPs

The toxicity of zirconia nanoparticles may differ based on several factors, including the specific cell lines used, the types of capping agents, and the nanoparticles' size and shape (Kumari et al., 2009). ZrO_2NPs adhere to macromolecules like proteins on the tumor surface and subsequently enter the tumor cells (Muthulakshmi et al., 2023a). According to Table 3, a limited number of studies have assessed the cytopathic effect of green ZrO_2NPs from *Parkia biglandulosa*, and *Nephelium lappaceum* fruit extract against the breast cancer cell lines (MCF-7) , (Muthulakshmi et al., 2023b) and (Saraswathi & Santhakumar, 2017), respectively. Consequently, additional research on the anticancer potentialities of green ZrO_2NPs is necessary.

Table 3 Biomedical applications of the biosynthesized zirconium nanoparticles

Green producer	Activity	Target	Finding	Reference
Azadirachita indica (leaf extract)	Antibacterial	Gram-negative (Escherichia coli)	An inhibition zone of 18mm was observed.	Singh et al. (2025)
Murraya koenigii (leaf extract)	Antibacterial	Gram negative (*E. coli*) and Gram positive (*Streptococcus aureus*)	ZrO_2 concentration of100 µg/paper disc exhibited the highest inhibition zone for both bacteria.	Chelliah et al. (2023)
Garlic & ginger (extracts)	Antibacterial	Gram positive *S. aureus*	The zone of inhibition was 10mm at a ZrONPs concentration of 200mg/ml.	Chowdhury et al. (2023)
Parkia biglandulosa (leaf extract)	Antibacterial	*Lactobacillus acidophilus, S. albus* and *S. mutans*	The inhibition zone against *L. acidophilus* was 28 mm, against *S. albus* was 26mm and against *S. mutans* was 32 mm, all at a 75µg/ml of ZrO_2NP_s	Muthulakshmi et al. (2023a)
Guettarda speciosa (leaf extract)	Antibacterial	Gram negative (*E. coli, Salmonella typhi, Pseudomonas aeruginosa* and *Proteus vulgaris*) and Gram-positive (*Bacillus subtilis*)	The zone of inhibition against E. coli was 10mm), against *B. subtilis* was 10mm, against *S. typhi* was 15 mm, against *P. vulgaris* was 5 mm and against *P. aeruginosa* was 8.5 mm, all at a 10µg/ml of ZrO_2 NPs.	Muthulakshmi et al. (2023b)
Annona reticulata (leaf extract)	Antibacterial	Gram negative (*Salmonella typhi*)	Growth inhibition was 78.2% at a ZrO2 NPs concentration of 100µg/ml.	Selvam et al. (2023)
Wrightia tinctoria (leaf extract)	Antibacterial	Gram negative (*E. coli*, *P. aeruginosa*) and Gram positive (*S. aureus* and *B. subtilis)*	The inhibition zone against *E. coli* was 22mm, against P. *aeruginosa* was 21mm, against S. *aureus* was 21 mm, and against *B. subtilis* was 20mm, all at a 10µg/ml of ZrO_2 NPs.	Al-Zaqri et al. (2021)
Helianthus annuus (seed extract)	Antibacterial	Gram negative (*E. coli* and *P. aeruginosa*) and Gram positive *(S. aureus* and *Klebsiella pneumoniae*)	The zone of inhibition against *E. coli* was 13mm, against *P. aeruginosa* was 13.5mm, against *S. aureus* was 12.0mm, and against *K. pneumoniae* was 12.5mm, all at a 100µg/ml of ZrO_2 NPs.	Goyal et al. (2021)
Penicillium spp. (culture supernatant)	Antibacterial	Gram negative (*E. coli* and *P. aeruginosa*) and Gram positive (*S. aureus*)	Minimum inhibitory concentration for *E. coli* was 0.75mM, and for *P. aeruginosa* was 0.375mM, but not recorded for *S. aureus*.	Ghomi et al. (2019)

Table 3. Cont.

Green producer	Activity	Target	Finding	Reference
Nyctanthes arbor-tristis (flower extract)	Antibacterial	Gram negative (*E. coli*), Gram positive (*S. aureus*)	The inhibition zone against *E. coli* was 17mm, and against *S. aureus* was 15mm for ZrO_2NPs at a ZrO_2NPs treated cotton (3%).	Gowri et al. (2015)
Enterobacter sp. (culture supernatant)	Antifungal	*Pezicula versicolor*	The antifungal inhibition zone for *Pezicula versicolor* was 25.18mm at a 20µg/ml of ZrO_2 NPs.	Ahmed et al. (2021a)
Phyllanthus niruri (leaf extract)	Antibacterial& antifungal	Gram negative (*E. coli*), Gram positive (*K. pneumoniae, B. subtilis* and *S. aureus*) and *Aspergillus niger*	Inhibition zone against *B. subtilius* was 15 mm, against *S. aureus was* 14mm, against *E. coli* was 14 mm, against *K. pneumoniae was* 14 mmm and against *A. niger* was 13 mm, all at a 200µg/ml of ZrO_2 NPs.	Yuan et al. (2022)
Laurus nobilis (leaf extract)	Antibacterial& antifungal	Gram negative (*K. pneumonia, E. coli*), Gram positive (*B. subtilis* and *S. aureus*), and *A. niger*	Inhibition zone against *B. subtilis* was 14mm, against *S. aureus* was 13mm, against *K. pneumonia* was 15 mm, against *E. coli* was 14mm, and against *A. niger* was 15mm, all at a 200µg/ml of ZrO_2 NPs.	Chau et al. (2023)
Aloe vera (leaf extract)	Antibacterial& antifungal	Gram negative (*E. coli*), Gram positive (*S. aureus*), *A. niger* and *Candida albicans*	The inhibition zone against *E. coli* was 32mm, against *S. aureus* was 23mm, against *A. niger* was 18 mm and against *C. albicans* was 22mm, all at a ZrO_2NPs treated cotton 3%.	Gowri et al. (2014)
Thymus vulgaris (extract)	Antibacterial, antifungal & Anticancer	Gram positive (*Bacillus* sp. and *Klebsiella* sp.), *Candida* sp. Breast cancer cell lines (MCF-7)	The inhibition zone against *Bacillus* sp. was 25mm, against *Klebsiella* sp. was 24mm, and against *candida* was 11mm, all at a ZrO_2NPs concentration of 100% mg/ml, IC_{50} values of ZrO_2NPs for MCF-7 was 21.35µg/ml.	Tharp & Karem (2024)
Parkia biglandulosa (leaf extract)	Anticancer	Breast cancer cell lines (MCF-7)	IC_{50} values of ZrO_2NPs for MCF-7 was 31.80µg/ml.	Muthulakshmi et al. (2023a)
Lagerstroemia speciosa (leaf extract)	Anticancer	Breast cancer cell lines (MCF-7)	The cells' viability with 18% inhibition was observed at 500µg/ml of zirconia nanoparticles.	Saraswathi & Santhakumar (2017)

Catalysis applications of biosynthesized ZrO_2NPs

Extensive literature reported the modification of zirconia nanoparticles by different agents to form zirconia based heterogeneous catalyst was used in transesterification and esterification of soybean oil to produce biodiesel (Xie & Wan, 2019). Moreover, extensive collection of studies recorded using the zirconia based heterogeneous catalyst in conversion of oleic acid into biodiesel (Zhang et al., 2020). Furthermore, the produced zirconia-based catalyst was employed for the transesterification of residual oil from cooking into biodiesel, yielding 79.7% (Omar & Amin, 2011). The transesterification of a non-palatable oil *Silybum marianum* using zirconia-based nanomaterials as a catalyst to formation biodiesel with a yield of 90.8% was also recorded (Takase et al., 2014). Additionally, zirconia based heterogeneous catalysts were used to transesterify tributyrin (Lu et al., 2020), respectively. Esterification of sunflower oil into biodiesel with a yield of 96.9 % was also recorded for the prepared zirconia-based nanoparticles (Dehghani & Haghighi, 2017).

Pollution control applications of biosynthesized ZrO_2NPs

Zirconium dioxide is a semiconductor with a wide bandgap and highly negative conduction band value, has shown promise as a photocatalyst due to its heat resistance, as well as its favorable optical and electrical properties (Kovalakova et al., 2020). ZrO_2NPs have been utilized in photocatalytic destruction of organic water contaminants including dyes and antibiotics (Kovalakova et al., 2020). The overuse of antibiotics has significantly contributed to the rise of antibiotic-resistant bacteria (Kovalakova et al., 2020). The majority of hospital wastewater is treated at independent treatment plants before being discharged into the drainage system (Yao et al., 2021). Consequently, effective methods for treating antibiotic pharmaceuticals in water are essential. In Table 4, the capacity of the biosynthesized ZrO_2NPs as antibiotic adsorbers is summarized. According to Al-nayili & Idan (2023), the biosynthesized ZrO_2NPs using *Sonchus asper* leaf extract demonstrated effective amoxicillin adsorption, achieving a capacity of 180.5mg/g and maintaining reusability over five cycles with 88.98% efficiency. Moreover, tetracycline adsorption capacity reached about 526.32 mg/g to the biosynthesized ZrO_2NPs by *Pseudomonas aeruginosa* culture supernatant at contact time of 15min (Debnath et al., 2020).

It is widely acknowledged that several textile dyes are pollutants. Research indicates that a significant quantity of textile dyes is discharged into water sources annually, resulting in several detrimental effects on human health (Zhou et al., 2019). Like antibiotics, many of these organic dyes are chemically unchangeable and resistant to phytodegradation (Nguyen et al., 2022). Both UV and visible light activate ZrO_2NPs for photocatalytic reactions, promoting electron excitation from the valence to conduction band, generating holes in the valence band, and leading to electron transfer to the surface, where they are captured by oxygen (Perumal et al., 2022). The vacant oxygen spaces hold the oxygen molecule, which leads to the formation of superoxide radicals (O_2). When oxygen molecules in the dye solution meet oxygen holes on the surface, they further transform into superoxide radicals then the generated radicals then interact with the pollutant, effectively degrading the target dye (Sugashini et al., 2022). In Table 5, the capacity of the biosynthesized ZrO_2NPs for dye degradation has been summarized.

Table 4 Antibiotic pollution management applications of the biosynthesized ZrO_2NPs

Green producer	Type of treatment	Pollutants finding	Reference
Sonchus asper (leaf extract)	Adsorption	Optimized amoxicillin adsorption occurs at a pH of 6, with a contact time of 250min and a capacity of 180.5mg/g, demonstrating reusability of up to 5 cycles (88.98%).	Al-nayili & Idan (2023)
Camellia snensis (leaf extract)	Photocatalytic degradation	The degradation of tetracycline using visible light occurred over an irradiation time of 240min, achieving a degradation efficiency of 80%.	Kumari et al. (2023)
Pseudomonas aeruginosa (culture supernatant)	Adsorption	Optimized tetracycline adsorption occurred at a pH of 6, with a contact time of 15min, a capacity of 526.32mg/g, and reusability of up to 5 cycles (81.55%).	Debnath et al. (2020)
Euclea natalensis (root extract)	Adsorption	Tetracycline adsorptive capacity recorded 30.45mg/g by response surface methodology.	da Silva et al. (2019)

Table 5 Textile dyes pollution management applications of the biosynthesized ZrO_2NPs

Green producer	Dye	Light source	Time of irradiation (min)	Degradation (%)	Reference
Azadirachita indica (leaf extract)	Methylene blue	Sunlight	180	67.4	Singh et al. (2025)
Murraya koenigii (leaf extract)	Methylene blue	Sunlight	20	94	Chelliah et al. (2023)
Annona reticulata (leaf extract)	Methylene blue	Sunlight	150	87.4	Selvam et al. (2023)
Sapindus mukorossi (pericarp extract)	Methylene blue	Without	300	94	Alagarsamy et al. (2022)
Phyllanthus niruri (leaf extract)	Methyl red, methyl orange, & methyl blue	Sunlight	6 h	74, 62 and 57, respectively	Yuan et al. (2022)
Wrightia tinctoria (leaf extract)	Reactive yellow 160 dye	Sunlight	120	94	Al-Zaqri et al. (2021)
Ficus elastica (leaf extract)	Rhodamine 6G	Sunlight	330	98.9	Haq et al. (2021)
Daphne alpine (leaf extract)	Methyl orange & picloram	Sunlight	75	76.94, 86, respectively	Rasheed et al. (2020)
Ficus benghalensis (leaf extract)	Methylene blue & methyl orange	UV light	240	91& 69, respectively	Shinde et al. (2018)
Lagerstroemia speciosa (leaf extract)	Methyl orange	Sunlight	290	94.5	Saraswathi & Santhakumar (2017)

The dye reduction efficiency of nanoparticles occurs in two stages: first, borohydride electrons accumulate on the NP surface, followed by the diffusion of organic dye molecules onto the surface, where they are reduced by the surface electrons (Basahel et al., 2015). Furthermore, UV light exposure generates electron-hole pairs that interact with dissolved oxygen molecules and surface hydroxyl groups, producing superoxide anion radicals and reactive hydroxyl radicals. (Shinde et al., 2018) . It has been hypothesized that the surface proteins of gold nanoparticles synthesized by *Cladosporium oxysporum* may enhance the adsorption of organic dyes, such as rhodamine B. These proteins can facilitate the formation of hydrophobic spaces by attaching amino acids to aromatic rings, which in turn improves the interaction between the dye and the nanocatalyst (Bhargava et al., 2016). ZrO_2NPs biosynthesized from *Ficus benghalensis* leaf extract achieved degradation rates of 61% for methylene blue dye and 91% for methylene orange dye under UV light irradiation (Shinde et al., 2018).

Other developing pollutants, like fluoride, have the potential to cause a range of serious health problems, including bone deformities, skeletal fluorosis, dental mottling and various neurological problems (Affonso et al., 2020). The use of hydrofluoric acid in chemical fertilization results in the generation of fluoride ions in water. Therefore, prior to being released from the aqueous medium, this pollutant must be treated. Therefore, this pollutant needs to be treated before being released into environment (Affonso et al., 2020). Fluorine ions were adsorbed at a rate of 98.55% by biosynthesized ZrO_2NPs from *Aloe vera* gel extract at a pH of 7 and a contact time of 15min, demonstrating a fluoride chemisorption capacity of 96.58mg/g (Prasad et al., 2014). Although previous studies have highlighted the effectiveness of ZrO_2NPs derived from biological sources in removing antibiotics, textile dyes, and fluoride, their potential for eliminating more recently identified contaminants, such as chlorinated compounds, heavy metal ions, and pharmaceuticals, has yet to be fully explored. Further research is needed to assess the efficacy of green ZrO_2NPs in addressing these emerging pollutants in the context of environmental cleanup.

ZrO_2-based nanocomposites applications.

Nanocomposites are composed of two or more distinct composites that possess distinct properties, often featuring separate phases divided by an interface. This combination gives nanocomposites unique properties that cannot be achieved by any of the individual components alone (Shameem et al., 2021). Nanocomposites can be sorted into three categories based on matrix type or host material used: ceramic matrix nanocomposites, metal matrix nanocomposites, and polymer matrix nanocomposites (Thinh et al., 2020).

The green synthesis of ZrO_2-based nanocomposites helps to overcome certain limitations of inherent ZrO_2 nanoparticles, such as bandgap energy and stability. To achieve a green and eco-friendly method, the synthesis of ZrO_2-based nanocomposites utilizes microbial or botanical sources, which are crucial in the processes of bioreduction, biocapping, and biostabilization for their transformation into composites. Table 6 provides a summary of the biotechnological applications of biosynthesized ZrO_2NPs nanocomposites.

The wide bandgap of ZrO_2NPs (~5.0eV) poses challenges in absorbing visible light, thereby limiting their potential for photocatalytic activities. However, modifications to these nanoparticles have been shown to effectively address this issue. ZrO_2-ZnO nanocomposites were biosynthesized using *Azadirachta indica* leaf extract with varying zirconia content (5%, 10%, & 15%) (Kay et al., 2023). The incorporation of ZrO_2NPs significantly altered the morphology of the nanocomposites, which could influence their properties and potential applications. Additionally, the band gap energy was reduced from 3.30eV to 3.15eV for ZnO_2NPs and from 3.93eV to 3.73eV for ZrO_2NPs, potentially enhancing the optical properties of the nanocomposites. This improvement makes them promising candidates for use in the manufacture of electronic and optical devices (Barman et al., 2023).

The incorporation of nickel into ZrO_2NPs using *Hevea brasiliensis* latex to form Ni-doped ZrO_2NPs has also been reported. This process resulted in a narrowed bandgap for the Ni-doped ZrO_2 nanocomposites, ranging from approximately 2.4 to 2.75eV, enhancing their potential for use in nanoelectronics. Using *Daphne alpine* leaf extract for the biosynthesis of V_2O_5/ZrO_2 nanocomposite resulted in improved bandgap energy and thermal stability (Rasheed et al., 2020).

Table 6 Various applications of biosynthesized zirconium nanoparticles nanocomposites

Green producer	Composites	Potential applications	Reference
Azadirachta indica (leaf extract)	ZrO_2-ZnO	Electronic and optical devices and water purification	Barman et al. (2023)
Azadirachta Indica (leaf extract)	$ZnZrO_3$	Exhibiting good thermal stability at high temperatures and promising potential for applications in electronics and catalysis	Kay et al. (2023)
Hevea brasiliensis latex	Ni-doped ZrO_2	Nanoelectronics	Yadav et al. (2022)
Ageratum conyzoides (leaf extract)	Ag/ZrO_2	The reduction of 2,4-dinitrophenylhydrazine, 4-nitrophenol, nigrosin and congo red.	Maham et al. (2020)
Daphne alpine (leaf extract)	V_2O_5/ZrO_2	The degradation efficiencies of V_2O_5/ZrO_2 were 76.9% for methyl orange and 86% for picloram, both achieved over a period of 75min	Rasheed et al. (2020)
Commelina diffusa (leaf extract)	Cu/ZrO_2	The reduction of 2,4-dinitrophenylhydrazine, Congo red, nigrosin, and methyl orange occurs at room temperature, characterized by extremely rapid reaction times	Hamad et al. (2019)
Centaurea cyanus (flower extract)	$Ag/Fe_3O_4/ZrO_2$	The reduction of 4-nitrophenol and methyl orange was achieved in three cycles, with a rapid reaction time of 7.5 to 8min	Rostami-Vartooni et al. (2019)
Justicia adhatoda (leaf extract)	CeO_2/ZrO_2	Antibacterial activity against *S. aureus*, and *E. coli*, antioxidant ability and anti-biofilm activities	Pandiyan et al. (2018)

This modification also facilitated better electron-hole separation, enhancing the degradation activities against methyl orange (76.9%) and picloram (86%). Doping with other transition metals such as Ag, Cu and Sm significantly alters the electronic characteristics and crystalline forms of the nanocomposites, enhancing their photocatalytic potentialities, recyclability, and stability. For instance, Cu/ZrO_2 nanocomposites (18–25nm) were synthesized using *Commelina diffusa* leaf extract, exhibiting excellent stability and promising capabilities for degrading compounds like 2,4-dinitrophenylhydrazine, Congo red, nigrosin and methyl orange, with remarkably fast reaction times ranging from 1 to 150 seconds (Hamad et al., 2019).

While green ZrO_2 nanoparticles exhibit exceptional catalytic activity, the separation and recovery of these non-magnetic tiny nanoparticles after their application can be challenging. To tackle this issue, the incorporation of magnetic components into zirconium nanoparticles to form nanocomposites has been proposed as a viable solution (Tran et al., 2022).

Other applications

Zirconia nanocoatings have been demonstrated in several studies to function as an efficient barrier that prevents corrosive ions from penetrating the substrate, improving the corrosion durability of mild steel plates (Kumar et al., 2017).

ZrO_2 nanoparticles synthesized using leaf extract of *Parkia biglandulosa* demonstrated significant corrosion inhibition properties. The results revealed that ZrO_2NPs can act as an effective corrosion inhibitor, achieving an inhibition efficiency of 99.26% (ZrC) when applied to mild steel, compared to the uncoated mild steel plate. Additionally, *Parkia biglandulosa* leaf extract was used to synthesis ZrO_2NPs, which showed notable corrosion inhibition capabilities. ZrO_2NPs can function as an efficient corrosion inhibitor, attaining an effectiveness of inhibition of 99.26% even at lower concentrations when applied to mild steel, compared to the uncoated mild steel plate (Muthulakshmi et al., 2023a).

The global need for cleaner, more sustainable energy is rising, and developing renewable energy sources is essential to meeting this demand (Vershinina et al., 2019). Solar radiation is the most plentiful renewable energy supply, so solar cells make it possible for people to easily access energy for inhabiting diverse locations worldwide. Other renewable energy sources that have been investigated recently include biomass, wind, hydro and geothermal energy (Nazeeruddin et al., 2011). The efficiency of dye-sensitized solar cells (DSSC) in converting solar energy can be improved by incorporating nanoparticles into certain components of the cell, which convert solar energy more efficiently (Solaiyammal & Murugakoothan, 2019).

The electrical properties of pellets (discs) made from biosynthesized ZrO_2NPs using *Citrus aurantifolia* fruit indicated that these pellets may have potential applications as electrolyte materials in intermediate-temperature solid oxide fuel cells (Majedi et al., 2016). Likewise, the biosynthesis of ZrO_2NPs using *Gloriosa superba* tuber powder enhanced the performance of photovoltaic systems by acting as effective components in the electrodes (Vennila et al., 2018).

Other applications demonstrated that green-synthesized zirconia nanoparticles using *Rosmarinus officinalis* leaf extract were incorporated as reinforcements in varying ratios into polyvinyl alcohol (PVA) thin films. The strength properties of the resulting nanocomposites indicated that the elastic modulus of 1 wt. % ZrO_2-PVA sample was approximately 5.5 times greater than that of the pure PVA thin film (Davar et al., 2018).

CONCLUSION AND CHALLENGES

The stringent standards of green chemistry are mostly not met by the chemical production of nanomaterials. The simplicity of synthesis, cost-effectiveness, environmental friendliness, and ease of scaling up make green approaches to nanomaterial synthesis extremely significant today, surpassing the drawbacks of traditional methods. One important area of biotechnology is the green production of NPs utilizing living organisms including bacteria, fungi, and plants. Since zirconia-based nanomaterials are widely used, the current study thoroughly investigates how various cultural and reaction parameters influence their composition, size, and shape. Greenly produced zirconium nanoparticles can be employed as antioxidants, antibacterial, and anticancer agents in a variety of biotechnological applications. Moreover, zirconium nanoparticles can be employed in many other fields such as bioremediative uses, food industries, intelligent farming, fabric manufacturing and sewage processing. ZnO_2NPs have drawn a lot of interest as prospective antibacterial agents because of their distinct physicochemical characteristics and wide-ranging efficacy against a variety of microbes including multidrug-resistant strains.

The main challenges encountered during zirconium nanoparticles biosynthesis are the creation of a certain size and shape particles through defined optimization conditions, conducting a comprehensive analysis of the metabolites or botanical extracts employed in the process of biosynthesis to understand the role of each compound in the process, and scaling-up production of these nanoparticles. Moreover, the stability of nanoparticles with high yields was linked to the optimization of factors including pH, precursor concentration, reaction time, and temperature. The use of green ZrO_2NPs in solar cells has been explored; however, the reaction mechanisms and methods to enhance energy harvesting efficiency remain insufficiently investigated. It is advisable to conduct further research in this area.

Funding: The authors extend their appreciation to the Deanship of Scientific Research at Northern Border University, Arar, KSA for funding this research work through the project number “NBU-FFR-2025-2902-02”.

Availability of data and materials: I don’t have any research data outside the submitted manuscript file.

Conflict of interest: The authors indicated no potential conflicts of interest.

Authors’ contributions: All authors shared writing, editing, and revising the MS and agree to its publication.

Ethical approval: Not applicable.

REFERENCES

Abdo, A.M., Fouda, A., Eid, A.M., Fahmy, N.M., Elsayed, A.M., Khalil, A.M.A., et al. (2021). Green synthesis of Zinc Oxide Nanoparticles (ZnONPs) by *Pseudomonas aeruginosa* and their activity against pathogenic microbes and common house mosquito, Culex pipiens. *Materials* 14: 6983. https://doi.org/10.3390/ma14226983

Abu-Tahon, M.A., Ghareib, M., Abdallah, W.E. (2020). Environmentally benign rapid biosynthesis of extracellular gold nanoparticles using *Aspergillus flavus* and their cytotoxic and catalytic activities. *Process Biochemistry* 95, 1-11.https://doi.org/10.1016/j.procbio.2020.04.015

Abu-Tahon, M.A., Alshammari, F.A., Shahhat, I.M., Ghareib, M., Abdallah, W.E. (2024). Eco-Friendly synthesis, characterization, and biomedical applications of biosynthesized bimetallic silver-gold nanoparticles by culture supernatant of *Aspergillus niger*. *Applied Biochemistry and Biotechnology*, 1-22. https://doi.org/10.1007/s12010-024-05035-w

Affonso, L.N., Marques Jr, J.L., Lima, V.V., Gonçalves, J.O., Barbosa, S.C., Primel, E.G., et al. (2020). Removal of fluoride from fertilizer industry effluent using carbon nanotubes stabilized in chitosan sponge. *Journal of Hazardous Materials:* 388: 122042. https://doi.org/10.1016/j.jhazmat.2020.122042

Ahmed, T., Ren, H., Noman, M., Shahid, M., Liu, M., Ali, M.A.,et al. (2021a). Green synthesis and characterization of zirconium oxide nanoparticles by using a native *Enterobacter* sp. and its antifungal activity against bayberry twig blight disease pathogen Pestalotiopsis versicolor. *Nano Impact* 21: 100281. https://doi.org/10.1016/j.impact.2020.100281

Ahmed, T., Wu, Z., Jiang, H., Luo, J., Noman, M., Shahid, M., et al. (2021b). Bioinspired green synthesis of zinc oxide nanoparticles from a native *Bacillus cereus* strain RNT6: characterization and antibacterial activity against rice panicle blight pathogens *Burkholderia glumae* and *B. gladioli. Nanomaterials,* 11: 884. https://doi.org/10.3390/nano11040884

Akintelu, S.A., Folorunso, A.S. (2020). A review on green synthesis of zinc oxide nanoparticles using plant extracts and biomedical applications. *BioNanoScience,* 10: 848-863. https://doi.org/10.1007/s12668-020-00774-6

Al-nayili, A., Idan, A.H. (2023). Environmentally friendly production, characterization, and utilization of ZrO2 nanoparticles for the adsorption of amoxicillin in water solutions. *Journal of Molecular Liquids,* 389: 122875. https://doi.org/10.1016/j.molliq.2023.122875

Al-Zaqri, N., Muthuvel, A., Jothibas, M., Alsalme, A., Alharthi, F.A., Mohana, V. (2021). Biosynthesis of zirconium oxide nanoparticles using *Wrightia tinctoria* leaf extract: characterization, photocatalytic degradation and antibacterial activities. *Inorganic Chemistry Communications,* 127: 108507. https://doi.org/10.1016/j.inoche.2021.108507

Alagarsamy, A., Chandrasekaran, S., Manikandan, A. (2022). Green synthesis and characterization studies of biogenic zirconium oxide (ZrO_2) nanoparticles for adsorptive removal of methylene blue dye. *Journal of Molecular Structure,* 1247: 131275. https://doi.org/10.1016/j.molstruc.2021.131275

Allaker, R., Vargas-Reus, M., Ren, G. (2012). Nanometals as antimicrobials. *Antimicrobial Polymers,* 2011: 327-350.

Bansal, V., Rautaray, D., Ahmad, A., Sastry, M. (2004). Biosynthesis of zirconia nanoparticles using the fungus *Fusarium oxysporum*. *Journal of Molecular Structure,* 14: 3303-3305.

Barman, S., Sikdar, S., Das, R. (2023). A comprehensive study on ZrO_2-ZnO nanocomposites synthesized by the plant-mediated green method. *Physica Scripta*, 98: 085947. https://doi.org/10.1088/1402-4896/ace857

Basahel, S.N., Ali, T.T., Mokhtar, M., Narasimharao, K. (2015). Influence of crystal structure of nanosized ZrO_2 on photocatalytic degradation of methyl orange. *Nanoscale Research Letters,* 10: 1-13.

Bhargava, A., Jain, N., Khan, M.A., Pareek, V., Dilip, R. V., et al. (2016). Utilizing metal tolerance potential of soil fungus for efficient synthesis of gold nanoparticles with superior catalytic activity for degradation of rhodamine B. *Journal of Environmental Management,* 183: 22-32.

Chau, T.P., Kandasamy, S., Chinnathambi, A., Alahmadi, T.A., Brindhadevi, K. (2023). Synthesis of zirconia nanoparticles using *Laurus nobilis* for use as an antimicrobial agent. *Applied Nanoscience*, 13: 1337-1344.

Chelliah, P., Wabaidur, S.M., Sharma, H.P., Majdi, H.S., Smait, D.A., Najm, M.A., et al. (2023). Photocatalytic organic contaminant degradation of green synthesized ZrO2 NPs and their antibacterial activities. *Separations* 10, 156. https://doi.org/10.3390/separations10030156

Chowdhury, M.A., Hossain, N., Mostofa, M.G., Mia, M.R., Tushar, M., Rana, M.M., et al. (2023). Green synthesis and characterization of zirconium nanoparticle for dental implant applications. *Heliyon,* 9(1): e12711.

da Silva, A.F.V., Fagundes, A.P., Macuvele, D.L.P., de Carvalho, E.F.U., Durazzo, M., Padoin, N., et al. (2019). Green synthesis of zirconia nanoparticles based on Euclea natalensis plant extract: Optimization of reaction conditions and evaluation of adsorptive properties. *Colloids Surfces A: Physicochemical and Engineering Aspects,* 583: 123915. https://doi.org/10.1016/j.colsurfa.2019.123915

Davar, F., Majedi, A., Mirzaei, A. (2018). Polyvinyl alcohol thin film reinforced by green synthesized zirconia nanoparticles. *Ceramics International,* 44: 19377-19382.

Debnath, B., Majumdar, M., Bhowmik, M., Bhowmik, K.L., Debnath, A., Roy, D.N. (2020). The effective adsorption of tetracycline onto zirconia nanoparticles synthesized by novel microbial green technology. *Journal of Environmental Management,* 261: 110235. https://doi.org/10.1016/j.jenvman.2020.110235

Dehghani, S., Haghighi, M. (2017). Sono-sulfated zirconia nanocatalyst supported on MCM-41 for biodiesel production from sunflower oil: Influence of ultrasound irradiation power on catalytic properties and performance. *Ultrasonics Sonochemistry,* 35: 142-151.

Din, M.I., Nabi, A.G., Rani, A., Aihetasham, A., Mukhtar, M. (2018). Single step green synthesis of stable nickel and nickel oxide nanoparticles from *Calotropis gigantea*: Catalytic and antimicrobial potentials. *Environmental Nanotechnology, Monitoring & Management,* 9: 29-36.

Elsayed, A., El-Shamy, G.M., Attia, A.A. (2022). Biosynthesis, characterization, and assessment of zirconia nanoparticles by *Fusarium oxysporum* species as potential novel antimicrobial and cytotoxic agents. *Egyptian Journal of Botany,* 62: 507-522.

Elshobary, M.E., Badawy, N.K., Ashraf, Y., Zatioun, A.A., Masriya, H.H., Ammar, M.M., et al. (2025). Combating antibiotic resistance: Mechanisms, multidrug-resistant pathogens, and novel therapeutic approaches: An updated review. *Pharmaceuticals*, 18(3): 402. https://doi.org/10.3390/ph18030402

Gayathri, V., Balan, R. (2021). Synthesis and characterization of pure Zirconium oxide (ZrO_2) nanoparticle by conventional precipitation method. *Journal of Environmental Nanotechnology*, 10(4): 19-21.

Ghareib, M., Abdallah, W., Tahon, M., Tallima, A. (2019a). Biosynthesis of copper oxide nanoparticles using the preformed biomass of *Aspergillus fumigatus* and their antibacterial and photocatalytic activities. *Digest Journal of Nanomaterials & Biostructures,* 14(2): 291-303.

Ghareib, M., Abu Tahon, M., Abdallah, W.E., Hussein, M. (2019b). Free radical scavenging activity of zinc oxide nanoparticles biosynthesised using *Aspergillus carneus*. *Micro & Nano Letters,* 14: 1157-1162.

Ghomi, A.R.G., Mohammadi-Khanaposhti, M., Vahidi, H., Kobarfard, F., Reza, M.A.S., et al. (2019). Fungus-mediated extracellular biosynthesis and characterization of zirconium nanoparticles using standard *Penicillium* species and their preliminary bactericidal potential: a novel biological approach to nanoparticle synthesis. *Iranian Journal of Pharmaceutical Research,* 18(4): 2101.

Gowri, S., Gandhi, R. R., Sundrarajan, M. (2014). Structural, optical, antibacterial and antifungal properties of zirconia nanoparticles by biobased protocol. *Journal of Materials Science & Technology,* 30: 782-790.

Gowri, S., Gandhi, R.R., Senthil, S., Sundrarajan, M. (2015). Effect of calcination temperature on nyctanthes plant mediated zirconia nanoparticles, optical and antibacterial activity for optimized zirconia. *Journal of Bionanoscience,* 9: 181-189.

Goyal, P., Bhardwaj, A., Mehta, B.K., Mehta, D. (2021). Research article green synthesis of zirconium oxide nanoparticles (ZrO_2NPs) using *Helianthus annuus* seed and their antimicrobial effects. *Journal of the Indian Chemical Society,* 98: 100089. https://doi.org/10.1016/j.jics.2021.100089

Hamad, S.M., Mahmud, S.A., Sajadi, S.M., Omar, Z. A. (2019). Biosynthesis of Cu/ZrO_2 nanocomposite using 7-hydroxy-4'-methoxy-isoflavon extracted from Commelina diffusa and evaluation of its catalytic activity. *Surfaces and Interfaces,* 15: 125-134.

Haq, S., Afsar, H., Din, I.U., Ahmad, P., Khandaker, M.U., Osman, H., et al. (2021). Enhanced photocatalytic activity of *Ficus elastica* mediated zinc oxide-zirconium dioxide nanocatalyst at elevated calcination temperature: Physicochemical study. *Catalysts,* 11: 1481. https://doi.org/10.3390/catal11121481

Hunter, R.J. (2013). "*Zeta Potential in Colloid Science: Principles and Applications*", Vol. 2. Academic Press.

Huq, M.A., Akter, S. (2021). Biosynthesis, characterization and antibacterial application of novel silver nanoparticles against drug resistant pathogenic *Klebsiella pneumoniae* and *Salmonella enteritidis*. *Molecules,* 26: 5996. https://doi.org/10.3390/molecules26195996

Huq, M.A., Apu, M.A.I., Ashrafudoulla, M., Rahman, M.M., Parvez, M.A.K., Balusamy, S.R., et al. (2023). Bioactive ZnO nanoparticles: Biosynthesis, characterization and potential antimicrobial applications. *Pharmaceutics,* 15: 2634. https://doi.org/10.3390/pharmaceutics15112634

Imanova, G.T., Agayev, T.N., Jabarov, S.H. (2021). Investigation of structural and optical properties of zirconia dioxide nanoparticles by radiation and thermal methods. *Modern Physics Letter B,* 35(02): 2150050. https://doi.org/10.1142/S0217984921500500

Kavitha, N., Venkatesh, K., Palani, N., Ilangovan, R. (2020). Synthesis and characterization of zirconium oxide nanoparticles using *Fusarium solani* extract. In: *AIP Conference Proceedings*, Vol. 2265. AIP Publishing. https://doi.org/10.1063/5.0017117

Kay, S.J.J., Chidhambaram, N., Thirumurugan, A., Gobalakrishnan, S. (2023). Environmentally benign *Azadirachta indica*-mediated green approach for the zinc zirconate nanocomposite synthesis: An alternative to the toxic chemical approach. *Inorganic Chemistry Communication,* 158: 111550. https://doi.org/10.1016/j.inoche.2023.111550

Khandel, P., Shahi, S.K. (2018). Mycogenic nanoparticles and their bio-prospective applications: status and future challenges. *Journal of Nanostructure in Chemistry,* 8: 369-391.

Kirubakaran, D., Wahid, J.B.A., Karmegam, N., Jeevika, R., Sellapillai, L., Rajkumar, M., et al. (2025). A comprehensive review on the green synthesis of nanoparticles: advancements in biomedical and environmental applications. *Biomedical Materials & Devices*, 1-26. https://doi.org/10.1007/s44174-025-00295-4

Kovalakova, P., Cizmas, L., McDonald, T.J., Marsalek, B., Feng, M., Sharma, V.K. (2020). Occurrence and toxicity of antibiotics in the aquatic environment: A review. *Chemosphere,* 251: 126351. https://doi.org/10.1016/j.chemosphere.2020.126351

Kumar, A.M., Babu, R.S., Ramakrishna, S., de Barros, A.L. (2017). Electrochemical synthesis and surface protection of polypyrrole-CeO_2 nanocomposite coatings on AA2024 alloy. *Synthetic Metals,* 234: 18-28.

Kumari, L., Li, W., Xu, J., Leblanc, R., Wang, D., Li, Y., et al. (2009). Controlled hydrothermal synthesis of zirconium oxide nanostructures and their optical properties. *Crystal Growth and Design,* 9: 3874-3880.

Kumari, N., Sareen, S., Verma, M., Sharma, S., Sharma, A., Sohal, H.S., et al. (2022). Zirconia-based nanomaterials: Recent developments in synthesis and applications. *Nanoscale Advances,* 4: 4210-4236.

Kumari, N., Anand, V., Sareen, S., Kondal, N., Aulakh, M.K., Sharma, A., et al. (2023). Synthesis of low-band gap porous zirconia nanoparticles via greener-route: Mechanistic investigation and their applications. *Materials Chemistry and Physics,* 294: 127004. https://doi.org/10.1016/j.matchemphys.2022.127004

Lu, N., Zhang, X., Yan, X., Pan, D., Fan, B., Li, R. (2020). Synthesis of novel mesoporous sulfated zirconia nanosheets derived from Zr-based metal-organic frameworks. *CrystEngComm,* 22: 44-51.

Maham, M., Nasrollahzadeh, M., Sajadi, S.M. (2020). Facile synthesis of Ag/ZrO_2 nanocomposite as a recyclable catalyst for the treatment of environmental pollutants. *Composites Part B: Engineering,* 185: 107783. https://doi.org/10.1016/j.compositesb.2020.107783

Majedi, A., Abbasi, A., Davar, F. (2016). Green synthesis of zirconia nanoparticles using the modified Pechini method and characterization of its optical and electrical properties. *Journal of Sol-Gel Science and Technology,* 77: 542-552.

Miu, B.A., Dinischiotu, A. (2022). New green approaches in nanoparticles synthesis: An overview. *Molecules,* 27: 6472. https://doi.org/10.3390/molecules27196472

Mohd Yusof, H., Mohamad, R., Zaidan, U.H., Abdul Rahman, N.A. (2019). Microbial synthesis of zinc oxide nanoparticles and their potential application as an antimicrobial agent and a feed supplement in animal industry: a review. *Journal of Animal Science and Biotechnology,* 10: 1-22.

Mourdikoudis, S., Pallares, R.M., Thanh, N.T. (2018). Characterization techniques for nanoparticles: comparison and complementarity upon studying nanoparticle properties. *Nanoscale,* 10: 12871-12934.

Muthulakshmi, N., Kathirvel, A., Senthil, M., Subramanian, R. (2023a). Green synthesis of zirconia nanoparticles and their characterization, anticancer activity and corrosion inhibition properties. *Journal of the Indian Chemical Society,* 100: 101076. https://doi.org/10.1016/j.jics.2023.101076

Muthulakshmi, N., Kathirvel, A., Subramanian, R., Senthil, M. (2023b). Biofabrication of zirconia nanoparticles: Synthesis spectral characterization and biological activity evaluation against pathogenic bacteria. *Biointerface Research in Applied Chemistry,* 13: 1-12.

Nazeeruddin, M.K., Baranoff, E., Grätzel, M. (2011). Dye-sensitized solar cells: A brief overview. *Solar Energy,* 85: 1172-1178.

Nguyen, L.T., Vo, D.-V. N., Nguyen, L.T., Duong, A.T., Nguyen, H.Q., Chu, N.M., et al. (2022). Synthesis, characterization, and application of $ZnFe_2O_4$@ZnO nanoparticles for photocatalytic degradation of Rhodamine B under visible-light illumination. *Environmental Technology and Innovation,* 25: 102130. https://doi.org/10.1016/j.eti.2021.102130

Omar, W.N.N.W., Amin, N.A.S. (2011). Biodiesel production from waste cooking oil over alkaline modified zirconia catalyst. *Fuel Processing Technology,* 92: 2397-2405.

Pandiyan, N., Murugesan, B., Sonamuthu, J., Samayanan, S., Mahalingam, S. (2018). Facile biological synthetic strategy to morphologically aligned CeO_2/ZrO_2 core nanoparticles using *Justicia adhatoda* extract and ionic liquid: Enhancement of its bio-medical properties. *Journal of Photochemistry and Photobiology B: Biology,* 178: 481-488.

Perumal, V., Inmozhi, C., Uthrakumar, R., Robert, R., Chandrasekar, M., Mohamed, S.B., et al. (2022). Enhancing the photocatalytic performance of surface-Treated SnO_2 hierarchical nanorods against methylene blue dye under solar irradiation and biological degradation. *Environmental Research,* 209: 112821. https://doi.org/10.1016/j.envres.2022.112821

Prasad, K.S., Amin, Y., Selvaraj, K. (2014). Defluoridation using biomimetically synthesized nano zirconium chitosan composite: Kinetic and equilibrium studies. *Journal of Hazardous Materials,* 276: 232-240.

Rasheed, P., Haq, S., Waseem, M., Rehman, S.U., Rehman, W., Bibi, N., et al. (2020). Green synthesis of vanadium oxide-zirconium oxide nanocomposite for the degradation of methyl orange and picloram. *Materials Research Express,* 7: 025011. https://doi.org/10.1088/2053-1591/ab6fa2

Reddy, G.B., Madhusudhan, A., Ramakrishna, D., Ayodhya, D., Venkatesham, M., et al. (2015). Green chemistry approach for the synthesis of gold nanoparticles with gum kondagogu: Characterization, catalytic and antibacterial activity. *Journal of Nanostructure in Chemistry,* 5: 185-193.

Rostami-Vartooni, A., Moradi-Saadatmand, A., Bagherzadeh, M., Mahdavi, M. (2019). Green synthesis of Ag/Fe_3O4/ZrO_2 nanocomposite using aqueous *Centaurea cyanus* flower extract and its catalytic application for reduction of organic pollutants. *Iranian Journal of Catalysis,* 9: 27-35.

Roy, A., Bulut, O., Some, S., Mandal, A.K., Yilmaz, M.D. (2019). Green synthesis of silver nanoparticles: Biomolecule-nanoparticle organizations targeting antimicrobial activity. *RSC Advances,* 9: 2673-2702.

Safaei, M., Moradpoor, H., Salmani Mobarakeh, M., Fallahnia, N. (2022). Optimization of antibacterial, structures, and thermal properties of Alginate-ZrO_2 bionanocomposite by the Taguchi method. *Journal of Nanotechnology,* 2022: 7406168. https://doi.org/10.1155/2022/7406168

Saif, S., Tahir, A., Chen, Y. (2016). Green synthesis of iron nanoparticles and their environmental applications and implications. *Nanomaterials,* 6: 209. https://doi.org/10.3390/nano6110209

Salem, S.S., Fouda, A. (2021). Green synthesis of metallic nanoparticles and their prospective biotechnological applications: An overview. *Biological Trace Element Research,* 199: 344-370.

Saraswathi, V.S., Santhakumar, K. (2017). Photocatalytic activity against azo dye and cytotoxicity on MCF-7 cell lines of zirconium oxide nanoparticle mediated using leaves of *Lagerstroemia speciosa*. *Journal of Photochemistry and Photobiology B: Biology,* 169: 47-55.

Selvam, K., Sudhakar, C., Selvankumar, T., Senthilkumar, B., Kim, W., Al-Ansari, M.M., et al. (2023). Photocatalytic degradation of malachite green and antibacterial potential of biomimetic-synthesized zirconium oxide nanoparticles using *Annona reticulata* leaf extract. *Applied Nanoscience,* 13: 2837-2843.

Shameem, M.M., Sasikanth, S., Annamalai, R., Raman, R.G. (2021). A brief review on polymer nanocomposites and its applications. *Materials Today: Proceedings,* 45: 2536-2539.

Shinde, H., Bhosale, T., Gavade, N., Babar, S., Kamble, R., Shirke, B., et al. (2018). Biosynthesis of ZrO_2 nanoparticles from *Ficus benghalensis* leaf extract for photocatalytic activity. *Journal of Materials Science: Materials in Electronics,* 29: 14055-14064.

Singh, A.K., Nakate, U.T. (2014) Microwave synthesis, characterization, and photoluminescence properties of nanocrystalline zirconia. *Scientific World Journal,* 1: 349457. https://doi.org/10.1155/2014/349457

Singh, A., Mohanta, V.L., Dahiya, S., Mishra, B.K. (2025). Biogenic synthesis of Azadirachta indica–mediated zirconium oxide nanoparticles: photocatalytic degradation of methylene blue and antimicrobial activity. *Biomass Conversion and Biorefinery,* 15(6): 8967-8981.

Solaiyammal, T., Murugakoothan, P. (2019). Green synthesis of Au and the impact of Au on the efficiency of TiO_2 based dye sensitized solar cells. *Materials Science for Energy Technologies,* 2: 171-180.

Sugashini, S., Gomathi, T., Devi, R.A., Sudha, P., Rambabu, K., Banat, F. (2022). Nanochitosan/carboxymethyl cellulose/TiO_2 biocomposite for visible-light-induced photocatalytic degradation of crystal violet dye. *Environmental Research,* 204: 112047. https://doi.org/10.1016/j.envres.2021.112047

Suriyaraj, S.P., Ramadoss, G., Chandraraj, K., Selvakumar, R. (2019). One pot facile green synthesis of crystalline bio-ZrO_2 nanoparticles using *Acinetobacter* sp. KCSI1 under room temperature. *Materials Science and Engineering: C,* 105: 110021. https://doi.org/10.1016/j.msec.2019.110021

Takase, M., Zhang, M., Feng, W., Chen, Y., Zhao, T., Cobbina, S.J., et al. (2014). Application of zirconia modified with KOH as heterogeneous solid base catalyst to new non-edible oil for biodiesel. *Energy Conversion and Management,* 80: 117-125.

Tharani, S.S.N. (2016). Green synthesis of zirconium dioxide (ZrO_2) nano particles using *Acalypha indica* leaf extract. *International Journal of Engineering and Applied Sciences,* 3(4): 257689.

Tharp, W.F., Karem, L.K.A. (2024). Green Synthesis, characterization, antimicrobial and anticancer studies of zirconium oxide nanoparticles using Thyme plant extract. *Moroccan Journal of Chemistry,* 12: 643-656.

Thinh, D.B., Tien, N.T., Dat, N.M., Phong, H.H.T., Giang, N.T.H., Oanh, D.T.Y., et al. (2020). Improved photodegradation of p-nitrophenol from water media using ternary $MgFe_2O_4$-doped TiO_2/reduced graphene oxide. *Synthetic Metals,* 270: 116583. https://doi.org/10.1016/j.synthmet.2020.116583

Tran, T.V., Nguyen, D.T.C., Kumar, P.S., Din, A.T.M., Jalil, A.A., Vo, D.-V.N. (2022). Green synthesis of ZrO_2 nanoparticles and nanocomposites for biomedical and environmental applications: A review. *Environmental Chemistry Letters*, 20, 1309–1331.

Uddin, I., Ahmad, A. (2016). Bioinspired eco-friendly synthesis of ZrO_2 nanoparticles. *Journal of Materials and Environmental Science,* 7: 3068-3075.

Usman, A.I., Aziz, A.A., Noqta, O.A. (2019). Green sonochemical synthesis of gold nanoparticles using palm oil leaves extracts. *Materials Today: Proceedings,* 7: 803-807.

Vennila, R., Kamaraj, P., Arthanareeswari, M., Sridharan, M., Sudha, G., Devikala, S., et al. (2018). Biosynthesis of ZrO nanoparticles and its natural dye sensitized solar cell studies. *Materials Today: Proceedings,* 5: 8691-8698.

Vershinina, K.Y., Dorokhov, V., Nyashina, G., Romanov, D. (2019). Environmental aspects and energy characteristics of the combustion of composite fuels based on peat, oil, and water. *Solid Fuel Chemistry,* 53: 294-302.

Weng, G., Li, W., Qin, F., Dong, M., Yue, S., Mehmood, S., et al. (2025). Eco-friendly synthesis of zirconia nanoparticles using *Sonchus asper* extract: A sustainable approach to enhancing Chinese cabbage growth and remediating chromium-contaminated soil. *Toxics*, 13(5): 324. https://doi.org/10.3390/toxics13050324

Xie, Q. (2025). Advances in microbial synthesis of metal nanoparticles and their environmental applications. *OAJRC Environmental Science,* 6(1): 1-13.

Xie, W., Wan, F. (2019). Immobilization of polyoxometalate-based sulfonated ionic liquids on UiO-66-2COOH metal-organic frameworks for biodiesel production via one-pot transesterification-esterification of acidic vegetable oils. *Chemical Engineering Journal,* 365: 40-50.

Yadav, L.R., Ramakrishnappa, T., Pereira, J.R., Venkatesh, R., Nagaraju, G. (2022). Rubber latex fuel extracted green biogenic nickel doped ZrO_2 nanoparticles and its resistivity. *Materials Today: Proceedings,* 49: 681-685.

Yao, S., Ye, J., Yang, Q., Hu, Y., Zhang, T., Jiang, L., et al. (2021). Occurrence and removal of antibiotics, antibiotic resistance genes, and bacterial communities in hospital wastewater. *Environmental Science and Pollution Research,* 28: 57321-57333.

Yazdanian, M., Rostamzadeh, P., Rahbar, M., Alam, M., Abbasi, K., Tahmasebi, E., et al. (2022). The potential application of green-synthesized metal nanoparticles in dentistry: A comprehensive review *Bioinorganic Chemistry and Applications*, 2022: 2311910. https://doi.org/10.1155/2022/2311910

Yuan, Y., Wu, Y., Suganthy, N., Shanmugam, S., Brindhadevi, K., Sabour, A., et al. (2022). Biosynthesis of zirconium nanoparticles (ZrO_2 NPs) by *Phyllanthus niruri* extract: Characterization and its photocatalytic dye degradation activity. *Food and Chemical Toxicology,* 168: 113340. https://doi.org/10.1016/j.fct.2022.113340

Zhang, Q., Lei, D., Luo, Q., Wang, J., Deng, T., Zhang, Y., Ma, P. (2020). Efficient biodiesel production from oleic acid using metal-organic framework encapsulated Zr-doped polyoxometalate nano-hybrids. *RSC Advances,* 10: 8766-8772.

Zhou, Y., Lu, J., Zhou, Y., Liu, Y. (2019). Recent advances for dyes removal using novel adsorbents: A review. *Environmental Pollution,* 252: 352-365.

Zinatloo-Ajabshir, S., Salavati-Niasari, M., (2016). Zirconia nanostructures: Novel facile surfactant-free preparation and characterization, *International Journal of Applied Ceramic Technology,* 13(1): 108–115.